Validation of a Controlled Reception Pattern Antenna (CRPA) Receiver Built from Inexpensive General-purpose Elements During Several Live Jamming Test Campaigns

Yu-Hsuan Chen, *Stanford University*
Sherman Lo, *Stanford University*
Dennis M. Akos, *University of Colorado at Boulder*
David S. De Lorenzo**,** *Stanford University*
Per Enge, *Stanford University*

BIOGRAPHY

Yu-Hsuan Chen is a Postdoctoral Scholar in the Stanford GPS Laboratory. He received his Ph. D in electrical engineering from National Cheng Kung University, Taiwan in 2011. His research interests include real-time GNSS software receiver and antenna array processing.

Sherman Lo is currently a senior research engineer at the Stanford GPS Laboratory. He is the Associate Investigator for the Stanford University efforts on the FAA evaluation of alternative position navigation and timing (APNT) systems for aviation. He received the Ph.D. in Aeronautics and Astronautics from Stanford University.

Dennis M. Akos obtained the Ph.D. degree from Ohio University in 1997. He is an associate professor with the Aerospace Engineering Science Department at University of Colorado at Boulder with visiting appointments at Luleå Technical University and Stanford University.

David S. De Lorenzo is a Principal Research Engineer at Polaris Wireless and a consulting Research Associate to the Stanford GPS Laboratory. His current research is in adaptive signal processing, software-defined radios, and navigation system security and integrity. He received the Ph.D. degree in Aeronautics and Astronautics from Stanford University and previously has worked for Lockheed Martin and for the Intel Corporation.

Per Enge is a professor of Aeronautics and Astronautics at Stanford University, where he is the Kleiner-Perkins Professor in the School of Engineering. He directs the Stanford GPS Laboratory, which develops satellite navigation systems. He has been involved in the development of the Federal Aviation Administration's GPS Wide Area Augmentation System (WAAS) and Local Area Augmentation System (LAAS).

ABSTRACT

The Controlled Reception Pattern Antenna (CRPA) is an effective approach for rejecting radio frequency interference. Conventionally, the dedicated CRPA antenna and hardware are usually precisely manufactured and calibrated carefully. The computational/processing requirement is always a major challenge for implementing a CRPA receiver. Even more demanding would be to incorporate the flexibility of the Software-Defined Radio (SDR) design philosophy in such an implementation. The Stanford University (SU) CRPA receiver development tackles these challenges to try to demonstrate the feasibility of a low cost commercial implementation by leveraging a SDR using Commercial Off-the-Shelf (COTS) components. This paper will discuss our real-time implementation of a COTS CRPA software receiver, its performance under numerous jamming conditions, and the lessons learned from these various trials. The developed CRPA receiver was tested in the live-jamming exercises in the US and Sweden. The scenarios include 1) dynamic jammers 2) static/multiple jammers in the various locations 3) different jammer types.

This paper shows the test results including the C/No improvement. From these results, we can see the benefit of our implementation compared to a commercial receiver. We also "replay" the signal from the collected data sets. With this replay functionality, the signal from a

single antenna and the composite signals by MVDR/power minimization algorithms are transmitted to commercial high-sensitivity GPS receiver. The replay results give us a true comparison between different algorithms/platforms.

INTRODUCTION

Global Navigation Satellite System (GNSS) signals are relatively weak and thus vulnerable to deliberate or unintentional interference. An electronically-steered antenna array system provides an effective approach to mitigate interference by controlling the reception pattern and steering beams/nulls. As a result, so-called Controlled Reception Pattern Antenna (CRPA) arrays have been deployed by organizations such as the US Department of Defense which seeks high levels of interference rejection.

As GNSS is being increasing relied upon and integrated into society, CRPA technology offers an important capability to the civil community. CRPA technology would provide robustness to critical infrastructure that relies on GNSS for timing such as cellular communication, and the power grid. This is important as deliberate interference on GNSS is increasing. Its use faces some major drawbacks such as cost and complexity. Furthermore, CRPA was developed for military use and the technology remains mostly in that domain. It has been primarily a restricted technology.

Our efforts have focused on developing a commercially viable CRPA system using Commercial Off-The-Shelf (COTS) components to support the needs of Federal Aviation Administration (FAA) alternative position navigation and timing (APNT) efforts. In our previous work on the CRPA receiver, two versions of the software and a study on array geometry have been done. In 2010, we implemented a 7-element, 2-bit-resolution, single-beam and real-time CRPA software receiver under Windows 7 [1]. The first version provided us experience on implementing the CRPA algorithms in a software receiver platform. However, it did not have enough dynamic range in the front-end. In 2011, the receiver was upgraded to support data collections with 14-bit-resolution, and from 4 antenna elements. It was capable of processing the data and steering twelve beams simultaneous in real time. However, the implementation, also under Windows 7, could only perform CRPA in post-processing mode due to the interaction of the data collection with Windows [2]. In 2012, we conducted a study to investigate the antenna array geometry and COTS antenna usage for the CRPA [3]. In this study, we created a self-calibration procedure to use antenna arrays built from COTS elements. And, we built a signal collection hardware consisting of four Universal Software Radio Peripheral 2 (USRP2) [4] and one host Personal Computer (PC)

Leveraging on our prior work on the CRPA receiver, a real-time CRPA software receiver under Ubuntu/Linux was developed with following features: 1) high dynamic range with 14-bit-resolution 2) all-in-view 12-channel pre-correlation beamforming 3) built using inexpensive COTS components including antenna and hardware 4) beamforming and nulling using Minimum Variance Distortionless Response (MVDR) and power minimization (PM) algorithms 5) calibrating array geometry and cable delay during runtime 6) temporal processing for frequency nulling.

In order to validate the anti-jam (A/J) performance of the Stanford University (SU) CRPA software receiver, the receiver was taken to three live-jamming tests in 2012. These tests generally included numerous different jamming scenarios and included dynamic and static jammers. The dynamic scenarios allowed for the demonstration of the fast updating rate of beamforming algorithm. Static single jammer power ramp scenarios allowed for a controlled demonstration of the maximum tolerable Jamming-to-Noise ratio (J/N) of the CRPA receiver. These scenarios quantified the robustness the SU CRPA receiver for different type of jammers. In scenarios with multiple static jammers, the ability of the CRPA receiver to mitigate several jammers from different directions was assessed. Another test was to demonstrate CRPA receiver capable of processing L5 signal and mitigate L5 interference in the form of a high-power Distance Measuring Equipment (DME) signal at 1173 MHz.

This paper is organized as follows. First, the hardware and software architecture of our CRPA software receiver are described. Then, an overview of field tests is given. For each test, the representative scenarios are described in detail and then test results are given between CRPA processing and single antenna commercial receiver. Finally, a summary of the work is presented.

HARDWARE ARCHITECTURE OF RECEIVER

The hardware architecture of CRPA software receiver is depicted in figure 1. The CRPA hardware contains a 4-element antenna array, four USRP2 software radio systems [4] and one host computer with Solid-State Drive (SSD) and is shown in figure 3. The signal received from each antenna passes to a USRP2 board equipped with a DBSRX2 programmable mixing and down-conversion daughter board. The individual USRP2 boards are synchronized by a 10 MHz external common clock generator and a Pulse Per Second (PPS) signal. The USRP2s are controlled by a host computer running the Ubuntu distribution of Linux. The USRP Hardware Driver (UHD) [5] software is used to configure USRP2 and daughter boards such as sampling rate and RF center frequency. This flexible hardware set up supports a four

antenna signal collection system and real-time CRPA software receiver for either L1 or L5 frequencies. The radiofrequency (RF) signal from each antenna element is converted to a near zero Intermediate Frequency (IF) and digitized to 14-bit complex or in-phase and quadarature outputs (I & Q, respectively). The RF center frequency was set to 1575 MHz for L1 and 1176 MHz for L5. The sampling rate was set to 4 MHz for L1 and 20 MHz for L5. The host computer is equipped with 4-port Ethernet card to receive the entire digital IF data with one port dedicated to each USRP2. Then, the data is processed in real-time and/or stored into SSDs in the host computer.

The flexible set up and SDR implementation allowed for the use of different antenna elements and configurations. The elements of antenna array can be arranged in layout such as Y or square shapes. One tested COTS antenna array is seen in figure 2. The electrical layout of antenna array is calculated by a procedure described in [3].

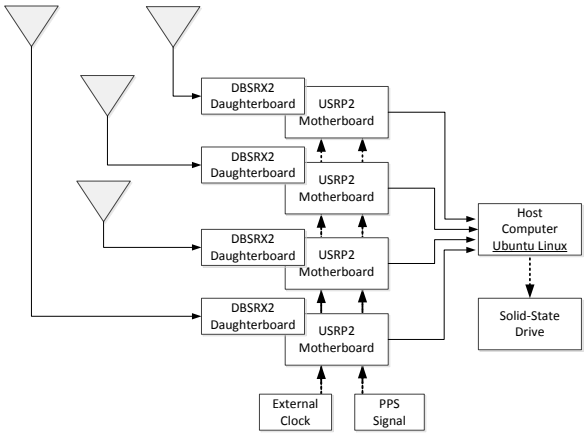

Figure 1. Block diagram of the CRPA software receiver hardware

Figure 2. Photo of the COTS antenna array

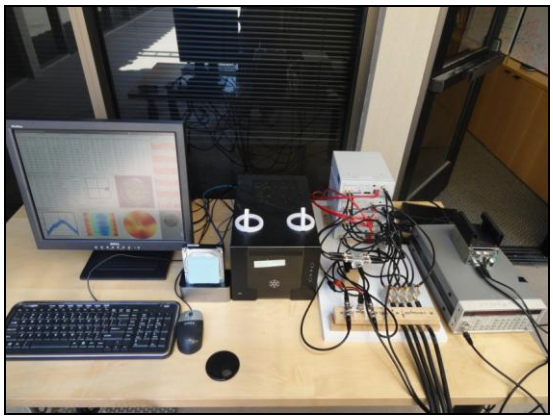

Figure 3. Photo of the CRPA software receiver hardware

SOFTWARE ARCHITECTURE OF RECEIVER

The software receiver [2][6][7][8][9] is developed in Eclipse with the GNU C compiler. Most of source code is programmed using C++. Assembly language is used to program the functions with high computational complexity such as correlation operations and weight-and-sum. The software architecture of CRPA software receiver is depicted in the figure 4. For each antenna element, a set of 12 tracking channels are processed. Each channel is dedicated to track the signal of single satellite. All the channels are processed in parallel. The tracking channels output carrier phase measurements to build the steering vectors for each satellite. Two algorithms, MVDR and power minimization, are adopted for calculating the weights adaptively. There are 13 sets of weights with 12 sets dedicated to each MVDR channel as a set is needed for each desired beam direction or satellite. One set used for power minimization which minimize output power without regard to satellite directions. The Space-Time Adaptive Processing (STAP) is also implemented with the weight calculation performed for each time tap. STAP provides enhanced anti-jamming performance both in the frequency and spatial domains. For the beamforming approach, the pre-correlation beamformer is adopted to form 13 composite signals by the multiplying weights with digital IF data and summed over all elements shown in figure 5. Each composite signal from MVDR is then processed by a single tracking channel. Moreover, the composite signal from PM is then processed by the other 12 tracking channels. Finally, positioning is performed after obtaining enough pseudoranges and navigation messages from MVDR channels.

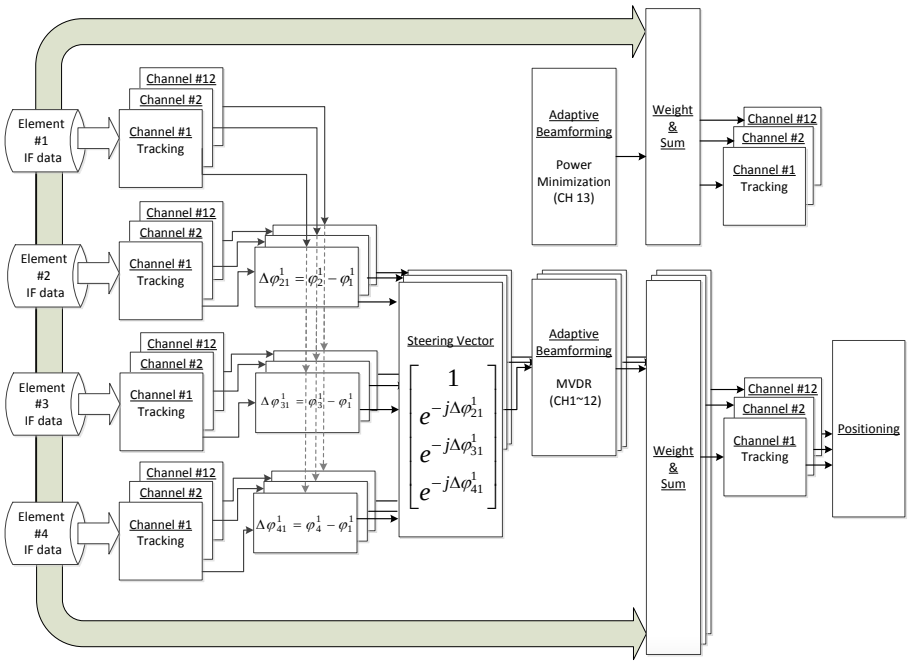

Figure 4. Block diagram of the software architecture

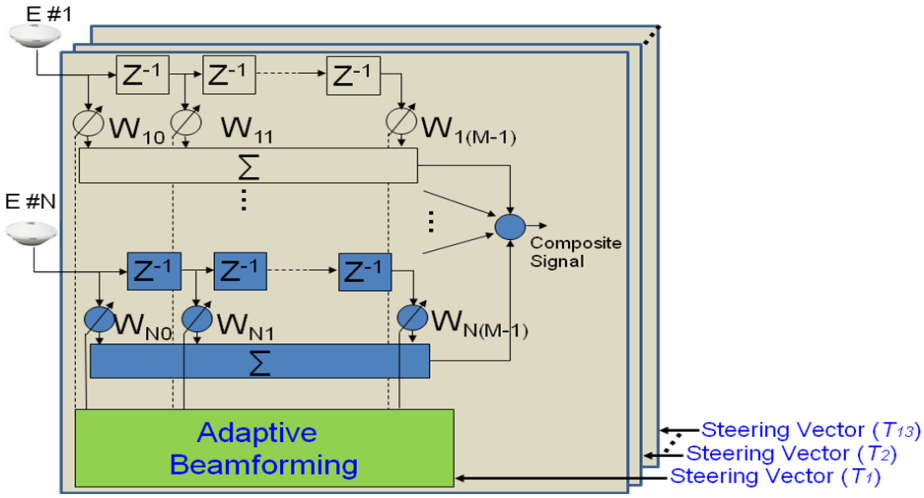

Figure 5. Architecture of Space-Time Adaptive Processing

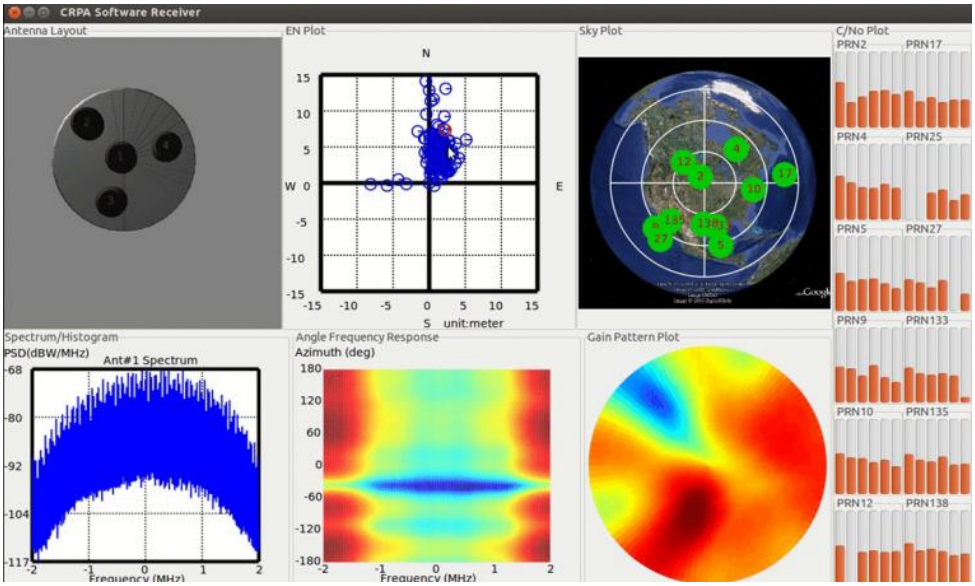

Figure 6. Screenshot of CRPA software receiver GUI

Figure 6 shows the graphical user interface (GUI) of CRPA software receiver. It includes several useful plots for showing receiver performance and jammer information. In this example, there is a jamming source in the direction of -45° azimuth as seen in the Gain Pattern Plot (there is a null in blue at this azimuth) or Angle Frequency Response plot. The Gain Pattern Plot is a composite of the gain pattern for all MVDR channels. Hence, it is useful for showing the nulls, which should be common to all channels, but not the beams, which depend on the satellite tracked in each channel. There is a deep null in the gain pattern as well as the angle-frequency response. The CRPA software receiver is tracking 12 satellites as seen in the C/No Plot. For each satellite (e.g. PRN 2) there are six columns indicating the C/No for different processing forms. Columns 1 and 2 are for MVDR and PM. Columns 3 to 6 are single antenna processing for antennas 1 to 4, respectively. Note that some of satellite channels lose lock because the jammer direction is close to satellite direction. These are the three processing approaches (MVDR, PM, and single antenna) that will be used to quantify the benefits of CRPA.

OVERVIEW OF FIELD TESTS

We participated in several live-jamming tests in 2012 and demonstrated the performance of the CRPA software receiver. Our general objectives are demonstrations of anti-jam performance in numerous scenarios, including comparison of different processing techniques and analyses of different hardware effects. Tests include two test campaigns and one self-test listed in table 1.

Table 1. Descriptions of tests

Name	Date	Location
DHS	June, 2012	White Sands, NM
Sweden	Oct, 2012	Robotförsöksplats Norrland (RFN), Sweden
Woodside	Nov, 2012	Woodside, CA

DHS TEST CAMPAIGN

The Department of Homeland Security sponsored the Gypsy jamming exercise in White Sands Missile Range (WSMR) in June, 2012. In this multi-day exercise, there were many dynamic and static scenarios. Dynamic jamming scenarios used multiple 250 milliWatt (mW) or 2.5 Watt (W) jammers on vehicles at approximately 40 miles per hour (mph). We sited our CRPA about 5 meters to the side of one of the main roads for the dynamic test scenarios. For static scenario, multiple 25 W jammers were operated from several locations throughout the test range. The CRPA was located in between several jammers to test the capability to reject multiple jammers with different direction.

A. DYNAMIC SCENARIOS

The dynamic scenario equipment set up placed the Stanford CRPA about 5 meters off a North-South running road traversed by up to two jamming vehicles. The location was near the turnaround point of the vehicles allowing for at least two jamming passes from each vehicle – a South bound and North bound pass. A separate Ublox receiver was also sited nearby. Due to the proximity of the CRPA to the road, the receiver experienced very strong jamming. This resulted in very low C/No during the short period of time when the vehicle passed by the antenna. Since the second jamming vehicle only trailed the first by a few minutes, there was little recovery time for re-acquisition between the first and second jammer. To better quantify the full benefits of the CRPA, the CRPA processed IF was input to a commercial high-sensitivity receiver (Ublox) in order to utilize the better C/No thresholds and fast re-acquisition of that receiver. In order to have a fair comparison between CRPA processing and a single antenna, all signals of interest (MVDR processed, PM processed and single antenna) were played back through a commercial high-sensitivity receiver shown in figure 7. The CRPA processing is the result of weight-and-sum from four antenna data sets to single data set and forms a CRPA processed IF signal.

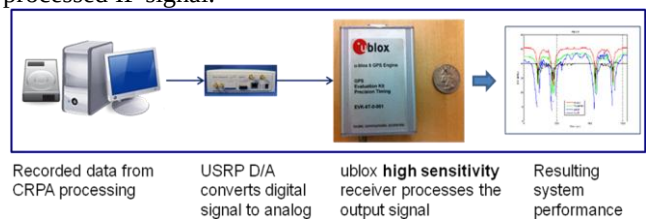

Figure 7. Playback procedure for comparing performance

Figure 8.
Left : jammer's path in the DHS dynamic scenario
Right : location of CRPA software receiver

The jammer's path and is shown in figure 8. Two 2.5W mobile jammers were separated by about four-minute. These vehicles passed by the SU CRPA twice each as

they turned around shortly after passing the test location. The comparison of C/No results and J/N is shown in figure 9. The blue curve shows the J/N which has four peaks of up to 32 dB due to the jammers' proximity to the CRPA. Three C/No curves are shown for performance and comparison. They are SU MVDR in red, SU PM in green and ublox single antenna in black. Figure 10 shows the C/No histogram of these three cases and their percent outage. The SU MVDR C/No has the highest C/No value due to a 6 dB gain from beamsteering and no outage of tracking. The Ublox single antenna C/No has lowest value and the most outages (7%).

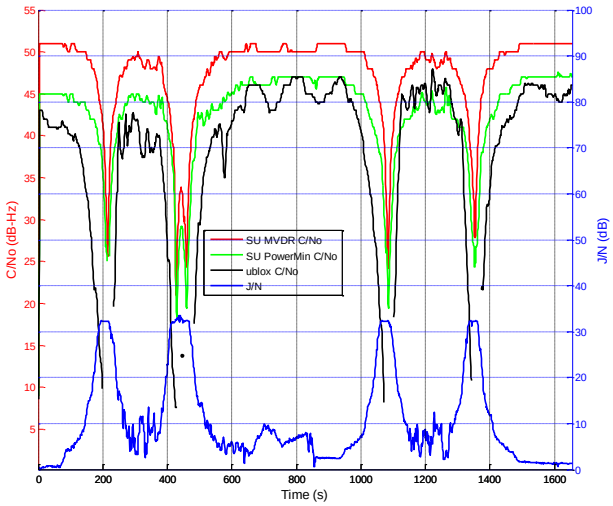

Figure 9. Comparison of C/No results and J/N in the DHS dynamic scenario

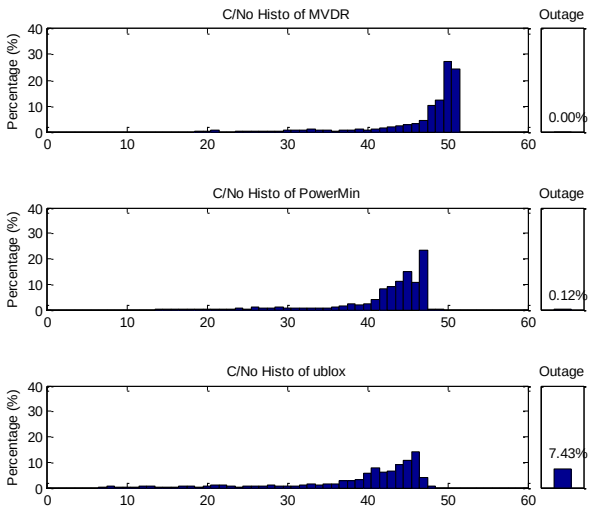

Figure 10. C/No histogram and outage in the DHS dynamic scenario

B. STATIC SCENARIOS

The static scenarios had jammers spread over the northern half of WSMR – an area of about 30 km in radius. From the SU test location, three jammers of the total six shown in the figure 11 were detected. The other jammers were blocked by mountainous terrain or too far from the test site. The jammers were turned on in sequential order. The first jammer was on in 50 second into the data collection. The others were on after around 680 second of data collecting. Figure 12 shows the composite gain pattern at the end of scenario. There are three deep nulls in the directions of three jammers. Figure 13 shows the C/No results along with the corresponding J/N. When the first jammer is on, there is no significant decrease in the C/No of each processing method. This is due to the low level of received jamming power. However, when other jammers are turned on with J/N increasing 10 dB, all C/No noticeably decrease though by different amounts. The single antenna drops the most - by about 8 dB. MVDR and PM drop 7 dB and 5 dB, respectively. The difference between CRPA and single antenna C/No during this jamming is less than the previous mobile scenario because the nulls need to be directed in three different directions resulting in nulls that are not as deep as before. A sense of the effect is seen in that PM has a smaller C/No drop than MVDR. PM has more degrees of freedom than MVDR since it is not constrained by beamsteering. So it can form slightly better nulls. However, it is important to note that MVDR still performs better as the beamsteering gain outweighs the slightly deeper nulls.

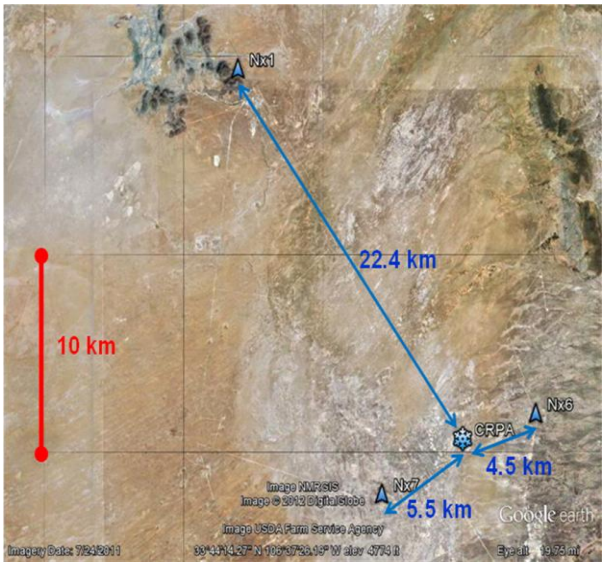

Figure 11. Map of jammers and CRPA software receiver in the DHS static scenario

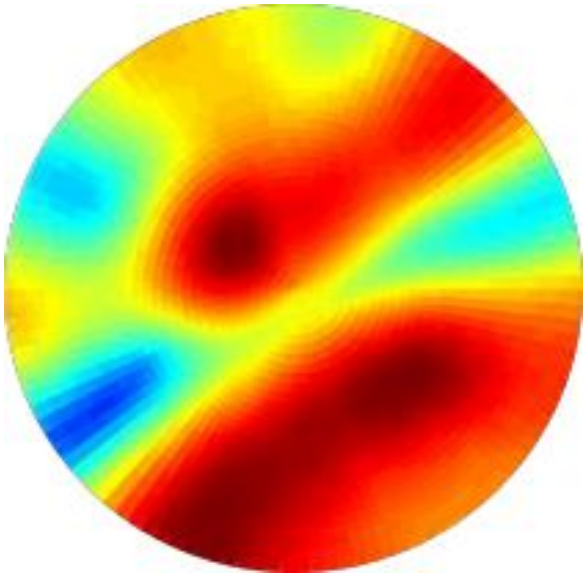

Figure 12. Gain pattern with three static jammers

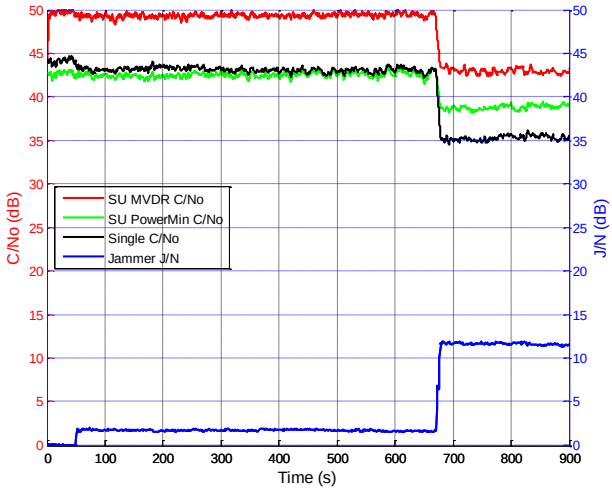

Figure 13. Comparison of C/No results and J/N in the DHS static scenario

SWEDEN TEST CAMPAIGN

The Swedish jamming test in Oct 2012 had more powerful jammers up to 50 dB J/N and numerous types of jamming waveforms. There are several static scenarios using different type of jammers. Figure 14 shows location of the jammer and the SU CRPA. The distance between them is about 10 meters. The antenna array used in the Sweden testing is comprised of four commercial patch antennas, which were arranged in square or Y layout shown in figure 15. Some representative scenarios in which the jammer power ramps from 20 dB to 50 dB J/N are shown. Three types of jammer are used for test -- 1) swept CW 2) wideband noise 3) 2 MHz bandwidth. In these scenarios, the anti-jam capability of our CRPA software receiver is characterized in term of maximum tolerable J/N without losing lock.

Figure 14. Location of jammer and receiver in the Sweden testing

Figure 15. Antenna array used in the Sweden testing

The spectrums of three jammers are shown in the figures 16, 17 and 18. The C/No vs. J/N of three scenarios are shown in figures 19, 20 and 21. The C/No results of MVDR, PM and single antenna to a commercial receiver are compared. An overall summary of performance is listed in table 2. In conclusion, the CRPA processing can provide around 20 dB of gain in the anti-jam performance compared to single antenna receiver.

Table 2. Summary of maximum tolerable J/N

	Swept CW	Broadband Noise	2 MHz BW
MVDR	> 47 dB	46 dB	50 dB
PowerMin	> 47 dB	43 dB	47 dB
ublox	23 dB	23 dB	29 dB
Gain with CRPA	24 dB	20~23 dB	18~21 dB

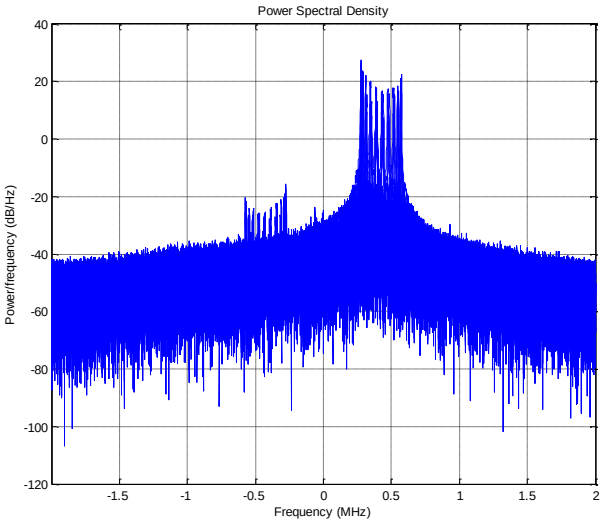

Figure 16. Spectrum of swept CW in the Sweden testing

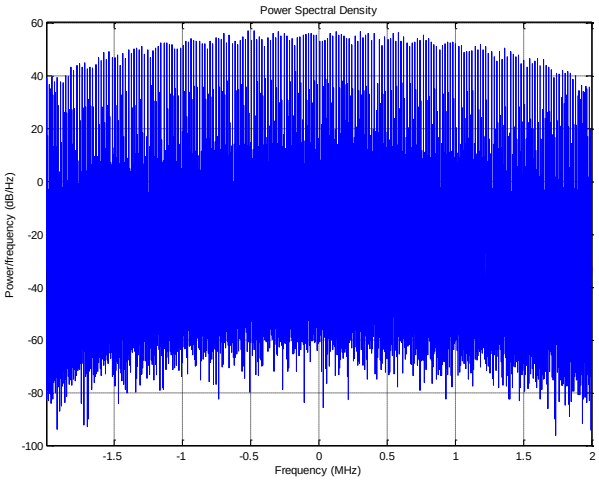

Figure 17. Spectrum of wideband noise in the Sweden testing

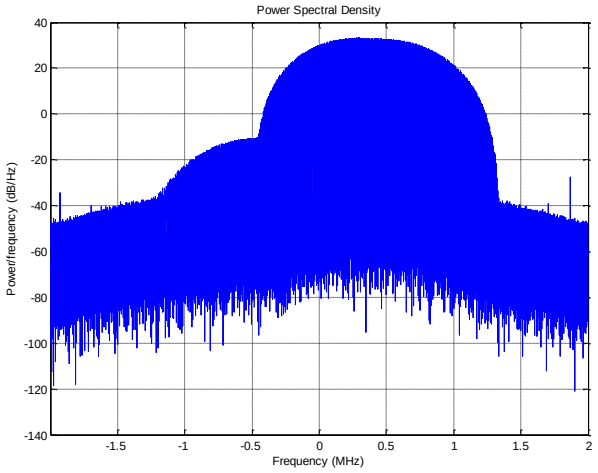

Figure 18. Spectrum of 2MHz bandwidth jammer in the Sweden testing

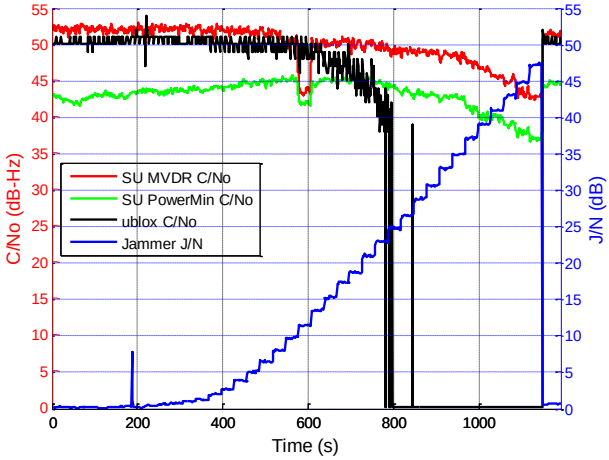

Figure 19. C/No vs. J/S of swept CW in the Sweden testing

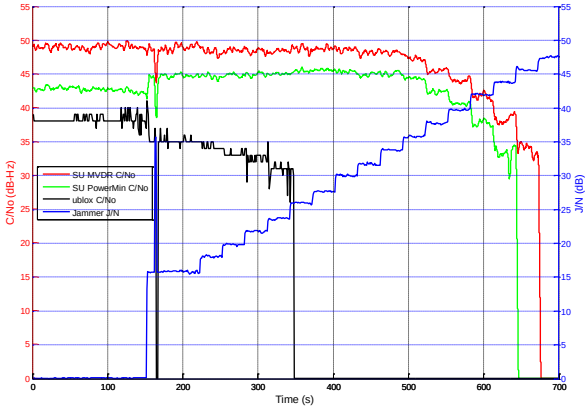

Figure 20. C/No vs. J/S of wideband noise in the Sweden testing

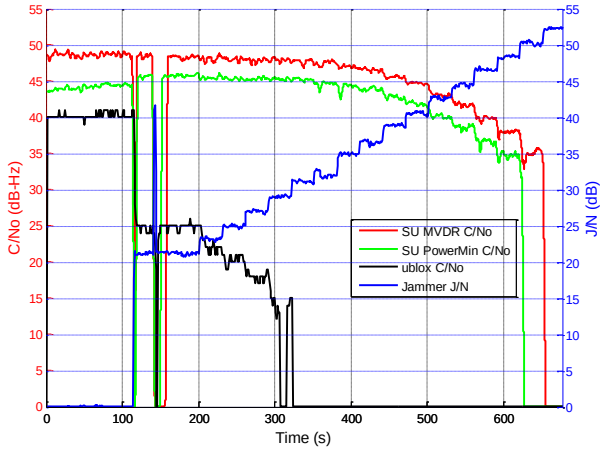

Figure 21. C/No vs. J/S of 2MHz bandwidth jammer in the Sweden testing

WOODSIDE L5 TEST

The SU CRPA was taken to Woodside VHF Omni direction Ranging (VOR)/Tactical Air Navigation (TACAN) (VORTAC) for testing as the DME portion of Woodside VORTAC (FAA identifier OSI) transmits on 1173 MHz, which is in the center of the GPS L5 band. Thus the test provided an opportunity to demonstrate the SU CRPA software receiver capability for operating on L5. Figure 22 shows a map of Woodside VORTAC with the location of the DME transponder. The figure also shows the antenna array which was placed only a few meters from the DME transponder. The antenna array utilized four Trimble Zephyr antennas and was arranged in a Y layout. Figure 23 shows the amplitude of GPS L5 collected signal with time. DME pulse pairs were present with 4% duty cycle over the duration of the collection. Because the antenna array was located only 5 meters away from the 100 W transponder, the DME pulse pairs saturated the USRP as seen in figure 24. The blue dash curve is the extrapolated DME pulse pair based on the received measurements. So the received signal in the red curve will saturate if the blue curve is beyond the saturation limit shown in black curve. However, the receiver still can track the L5 signals from three WAAS geostationary satellites (GEOs) and one GPS satellite, PRN 25, as seen in figure 25. Figure 26 shows the C/No vs. duty cycle of DME signal. The black curve is the playback result of single antenna data set to NovAtel OEMV-3 receiver. It takes about 25 seconds to acquire signal. After that, there is one dropout in the NovAtel single antenna C/No. The MVDR and PM C/No results show that CRPA processing allowed the receiver to remain in lock.

Figure 22. Left : satellite view of Woodside VORTAC Right : location of antenna array and DME transponder in Woodside

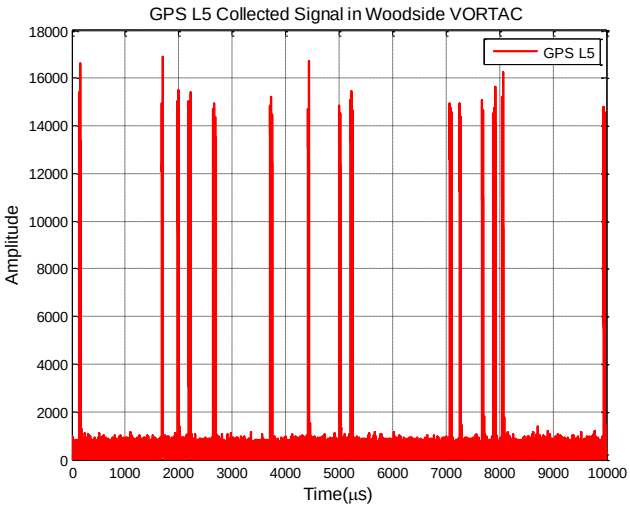

Figure 23. Amplitude of L5 collected signal in the Woodside testing

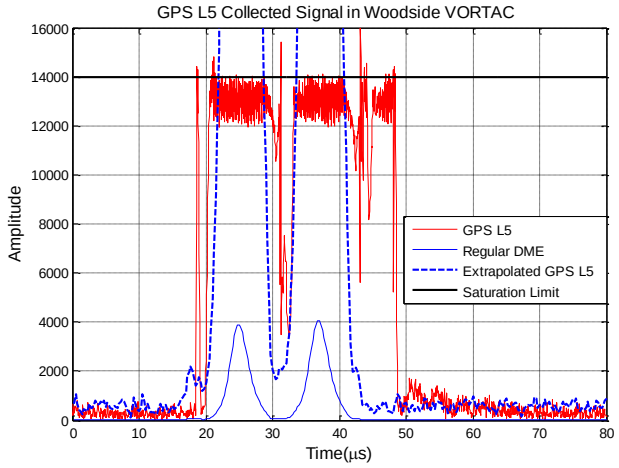

Figure 24. Amplitude of L5 collected signal compared to regular DME pulse pair

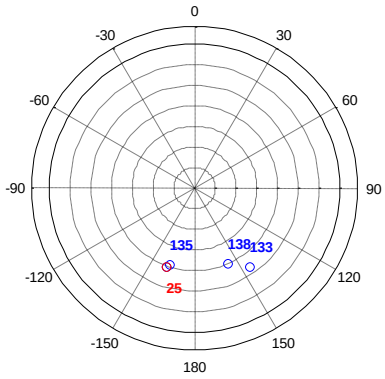

Figure 25. Skyplot of L5 in the Woodside testing

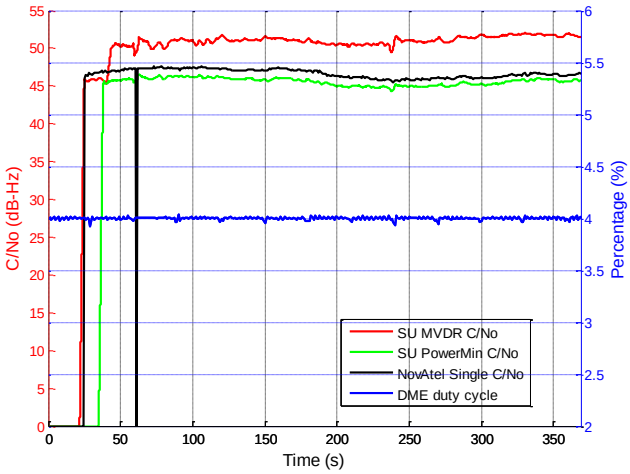

Figure 26. C/No vs. duty cycle of DME signal in the Woodside testing

SUMMARY

Stanford has designed and implemented a real-time CRPA software receiver using inexpensive COTS elements. This receiver has been validated in three field tests. The beam forming algorithms implemented in the receiver can rapidly update the gain pattern of antenna to null dynamic jammers moving at 200 degrees/second (40 mph at a distance of 5 meters) relative to the antenna. Our CRPA receiver has the capability to mitigate over 40 dB J/N jammers for three types 1) swept CW 2) broadband noise 3) 2MHz bandwidth. In comparison to a commercial single-antenna receiver, our CRPA software receiver can provide at least 20 dB gain for the anti-jam performance in these scenarios. We also successfully tested the CRPA receiver for processing the L5 signal under an environment with the pulse-type/high-power DME signal. This work is potentially the first real-time CRPA ever tested for L5 in the open literature. Additionally, the testing allow for the characterization of A/J performance of a commercial system using the latest technologies. A playback procedure was created to replay the signals from recorded and CRPA processed data. This procedure allowed for the combination of CRPA processing with the latest high sensitivity, fast reacquisition commercial receiver.

ACKNOWLEDGMENTS

The authors gratefully acknowledge of John K. Merrill and Michael Bergman from Department of Homeland Security (DHS) for organizing DHS jamming exercise. The authors gratefully acknowledge Fredrik Marsten Eklöf from Swedish Defense Research Agency for organizing the Sweden testing. The authors gratefully acknowledge Dan Specht from Federal Aviation Administration (FAA) for providing us access to the Woodside VORTAC facility. The authors gratefully acknowledge Gabriel Wong's assistance for replaying L5 signal to NovAtel Receiver. The authors gratefully acknowledge the FAA CRDA 12-G-003 for supporting this research.

REFERENCES

[1] Y.-H. Chen, D. S. De Lorenzo, J. Seo, S. Lo, J.-C. Juang, P. Enge, and D. M. Akos, "Real-Time Software Receiver for GPS Controlled Reception Pattern Array Processing," Proceedings of ION GNSS 2010, Portland, OR, September 2010, pp. 1932-1941.

[2] Y.-H. Chen, J.-C. Juang, J. Seo, S. Lo, D.M. Akos, D. S. De Lorenzo, P Enge, "Design and Implementation of Real-Time Software Radio for Anti-Interference GPS/WAAS Sensors," Sensors 2012, 12, pp. 13417-13440.

[3] Y.-H. Chen, "A Study of Geometry and Commercial Off-The-Shelf (COTS) Antennas for Controlled Reception Pattern Antenna (CRPA) Arrays," Proceedings of ION GNSS 2012, Nashville, TN, September 2012.

[4] USRP2 motherboard and DBSRX2 programmable daughterboard, Ettus Research LLC, reachable on the web at http://www.ettus.com.

[5] UHD - USRP Hardware Driver, Ettus Research LLC, reachable on the web at http://files.ettus.com/uhd_docs/manual/html/.

[6] U.S. Patent No. 7,305,021, "Real-Time Software Receiver," Awarded Dec. 4, 2007, by B.M. Ledvina, M.L. Psiaki, S.P. Powell, and P.M. Kintner, Jr.

[7] Y.-H. Chen and J.-C. Juang, "A GNSS Software Receiver Approach for the Processing of. Intermittent Data," Proceedings of ION GNSS 2007, 2007

[8] J. Seo, Y.-H. Chen, D. S. De Lorenzo, S. Lo, P. Enge, D. Akos, and J. Lee, "A Real-Time Capable Software-Defined Receiver Using GPU for Adaptive Anti-Jam GPS Sensors," Sensors 2011, 11, pp. 8966-8991

[9] P. Misra and P. Enge, Global Positioning System: Signals, Measurement, and Performance, 2nd Edition, Ganga-Jamuna Press, Lincoln, MA. , 2006